Electronic structure differences between H_2-, Fe-, Co-, and Cu-phthalocyanine highly oriented thin films observed using NEXAFS spectroscopy

T. M. Willey,[1,a)] M. Bagge-Hansen,[1] J. R. I. Lee,[1] R. Call,[1,2,b)] L. Landt,[1,3,c)] T. van Buuren,[1] C. Colesniuc,[4,d)] C. Monton,[4] I. Valmianski,[4] and Ivan K. Schuller[4]

[1]*Condensed Matter and Materials Division, Lawrence Livermore National Laboratory, California 94550, USA*
[2]*Department of Physics and Astronomy, Utah State University, Logan, Utah 84322, USA*
[3]*Institute for Optics and Atomic Physics, Technical University of Berlin, Berlin, Germany*
[4]*Department of Physics, University of California, San Diego, La Jolla, California 92093, USA*

(Received 8 November 2012; accepted 28 May 2013; published online 15 July 2013)

Phthalocyanines, a class of macrocyclic, square planar molecules, are extensively studied as semiconductor materials for chemical sensors, dye-sensitized solar cells, and other applications. In this study, we use angular dependent near-edge x-ray absorption fine structure (NEXAFS) spectroscopy as a quantitative probe of the orientation and electronic structure of H_2-, Fe-, Co-, and Cu-phthalocyanine molecular thin films. NEXAFS measurements at both the carbon and nitrogen K-edges reveal that phthalocyanine films deposited on sapphire have upright molecular orientations, while films up to 50 nm thick deposited on gold substrates contain prostrate molecules. Although great similarity is observed in the carbon and nitrogen K-edge NEXAFS spectra recorded for the films composed of prostrate molecules, the H_2-phthalocyanine exhibits the cleanest angular dependence due to its purely out-of-plane π^* resonances at the absorption onset. In contrast, organometallic-phthalocyanine nitrogen K-edges have a small in-plane resonance superimposed on this π^* region that is due to a transition into molecular orbitals interacting with the $3d_{x^2-y^2}$ empty state. NEXAFS spectra recorded at the metal L-edges for the prostrate films reveal dramatic variations in the angular dependence of specific resonances for the Cu-phthalocyanines compared with the Fe-, and Co-phthalocyanines. The Cu $L_{3,2}$ edge exhibits a strong in-plane resonance, attributed to its b_{1g} empty state with $d_{x^2-y^2}$ character at the Cu center. Conversely, the Fe- and Co- phthalocyanine $L_{3,2}$ edges have strong out-of-plane resonances; these are attributed to transitions into not only b_{1g} (d_{z^2}) but also e_g states with d_{xz} and d_{yz} character at the metal center. © *2013 AIP Publishing LLC*. [http://dx.doi.org/10.1063/1.4811487]

INTRODUCTION

Thin films of organometallic phthalocyanines (PCs) are versatile device materials with tunable electrical,[1,2] magnetic,[3,4] and structural[5,6] properties. These characteristics make phthalocyanines suitable for applications in dye-sensitized solar cells,[7,8] organic transistors,[9–13] chemiresistive gas-sensors,[14–17] and organic light emitting diodes.[18] The broad success in implementing this class of planar, organic molecules is a direct consequence of the tunability and sensitivity of their electronic and optical properties with gap energies corresponding to visible wavelengths. In thin film configurations, specified device performance is achieved through a combination of structural selectivity, and the choice of metal center atom. Nearly all transition metals and many heavier elements can reside at the relatively stable square planar center of the phthalocyanine. The metal atom interacts with the ligand, giving rise to a coordination complex with distinct electronic structure.

Building a clear understanding of phthalocyanine electronic structure, especially the nature of metal-ligand interactions, is a fundamental prerequisite to organoelectronic device engineering. Of particular significance are first row transition organometallic phthalocyanines, including Fe-, Co-, and Cu-PCs investigated here (Fig. 1), where systematic electronic structure changes occur with increasing d-electron filling. Numerous efforts have been made to characterize and model the electronic structure of these organometallic PCs.[1,2,19] Meanwhile, improvements in deposition techniques have enabled experimental studies of highly oriented, thin films (typically <25 nm thick) on a variety of single crystal substrates, e.g., Au.[20–29] High quality films prepared with advanced deposition techniques have been investigated by a variety of methods, including x-ray diffraction (XRD),[5,30] scanning tunneling microscopy (STM),[31–33] inverse photoemission spectroscopy (IPES),[28,34,35] x-ray photoemission spectroscopy (XPS),[20,21,36] ultra-violet photoemission spectroscopy (UPS),[36] and near-edge x-ray absorption fine structure (NEXAFS).[21–23,26,29,37–44] Of these experimental methods, NEXAFS has consistently demonstrated success in revealing both local electronic structure (i.e., unoccupied molecular orbitals) and the orientation of condensed molecular films.[23,24,29,37,38,42–51] Thin films of PCs with highly controlled relative molecular orientation,

a)Author to whom correspondence should be addressed. Electronic mail: willey1@llnl.gov
b)Current address: Department of Physics and Astronomy, University of North Carolina, Chapel Hill, North Carolina 27599, USA.
c)Current address: Li-Tec Battery GmbH, Dresden, Germany.
d)Current address: Intel Corporation, Hillsboro, Oregon, 97124, USA.

with respect to the chosen substrate, are ideal candidates for NEXAFS. The planar geometry and sp^2 bonding of the PC molecules lead to transition dipole moments that are out-of-plane for the π^* orbitals, and in-plane for the C−C and C−N σ^* orbitals.[52] When coupled with the use of linearly polarized synchrotron soft x-rays, these distinct transition dipole moment orientations result in strong angular anisotropy of the C 1s and N 1s (K-edge) x-ray absorption resonance intensities for PC films with well-defined molecular orientation. By examining this angular dependence, the orientations of PC molecules are revealed. Due to the valuable structural information available from NEXAFS experiments at the C and N K-edges, the majority of prior studies of PC films have focused upon measurements at these edges. In contrast, comparatively fewer experiments have been reported for the metal 2p (L-edge) NEXAFS,[42,53–56] particularly studies which comprehensively combine the angular dependence of the $L_{3,2}$-edge spectra with the electronic and orientational information gained from the C and N K-edges, with direct comparison to computed angular-dependent x-ray absorption. Theoretical efforts, including a number of detailed *ab initio* calculations, are largely complementary to these data;[4,35,39–41,44,54,56–65] however, relatively little work has been conducted to extract explicit x-ray absorption cross-sections from entire molecules to predict angular-dependent NEXAFS.

To further understanding of these materials, a complete collection of angular dependent NEXAFS at the C K-edge, N K-edge, and metal $L_{3,2}$-edges were concurrently acquired on a series of highly oriented H_2- Fe-, Co-, and Cu- phthalocyanine thin films to determine the electronic structure near the metal center. This study combines the data acquired from ordered films with a robust theoretical analysis using a bespoke implementation of the StoBe Density Functional Theory (DFT) package to generate anisotropic x-ray absorption cross-sections and model the angular dependent NEXAFS at the C K-edge, N K-edge and particularly, the metal L_3-edges.

EXPERIMENTAL

All organometallic PCs [Fig. 1] were purchased from Sigma Aldrich, and purified several times in a gradient sublimation system, pumped to $\sim 1 \times 10^{-6}$ Torr and heated to 400°C in cycles of 24 h.[66] Thin films of PCs were deposited in an organic molecular beam deposition system. This deposition system is contained within an ultra-high vacuum (UHV) chamber with base pressure $<1 \times 10^{-10}$ Torr. Purified PCs were loaded into quartz crucibles in Knudsen cells and evaporated at temperatures between 300 and 450°C. Deposition rates of 0.3-0.4 Å/s were achieved by adjusting the temperature. Film thicknesses were monitored using a calibrated quartz crystal microbalance. Deposited PC thin films were 50 nm thick. Substrates were (0001) cut sapphire; Au coated substrates were prepared by evaporating 40 nm Au onto sapphire and annealing at 300°C for three hours to decrease surface roughness and promote grain enlargement.[66] Substrates were azimuthally rotated continuously during deposition to ensure uniform films.[66]

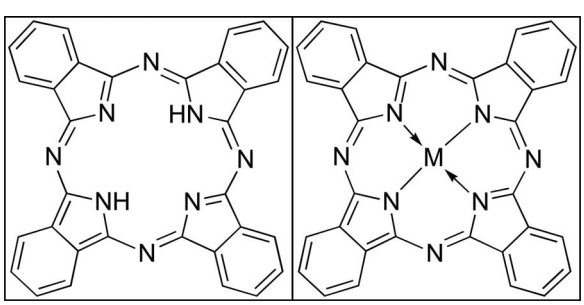

FIG. 1. H_2– (left) and organometallic (right) phthalocyanines; in this work, M = Cu, Co, and Fe. The NEXAFS transition dipole moments from 1s to σ^* orbitals lie in-plane along C−H, C−C, and C−N bonds, while the π^* resonances are normal to the molecular plane.

NEXAFS data were acquired at beamline 8.0 of the Advanced Light Source (ALS) and at beamline 8.2 at the Stanford Synchrotron Radiation Laboratory. At the ALS, the beam spot was defocused to about 4 mm^2 in order to reduce flux and associated beam-induced degradation. No beam damage was observed in the samples in the timeframe required to acquire the spectra. Total electron yield (TEY) spectra were acquired by measuring the sample drain current. All TEY spectra were normalized both to a concurrent, upstream, Au flux monitor, and subsequently to the intensity of the absorption step-edge. Total fluorescent yield (TFY) and Auger electron yield (AEY) were also measured, but are not shown for brevity. The AEY, TEY, and TFY detection modes have depth sensitivities of Angströms, nanometers, and hundreds of nm, respectively. All detection methods with varying depth sensitivity yielded NEXAFS data with similar angular-dependent intensity changes, indicating our substrates and deposition techniques led to uniform orientational arrangement throughout the films.

The mean spatial orientation of molecular films can be approximated through analysis of angular dependence in NEXAFS that arises from anisotropy in the transition probability for particular resonances. For PCs this is especially apparent for the C and N K-edge π^* and σ^* resonances where, for example, the 1s to π^* transition dipole moment is approximated by a single vector orthogonal to the phthalocyanine molecular plane,[35] or C 1s to σ^* dipole moments are approximated as vectors in the molecular plane. These lead to estimations of the molecular orientation through the relationships[35,37]

$$\frac{I_v(\Theta_i, \mathrm{A})}{I_v(\Theta_j, \mathrm{A})} = \frac{P(3\mathrm{A}-1)\Theta_i - \mathrm{A} + 1}{P(3\mathrm{A}-1)\Theta_j - \mathrm{A} + 1} \tag{1}$$

and

$$\frac{I_p(\Theta_i, \Gamma)}{I_p(\Theta_j, \Gamma)} = \frac{P(3\Gamma-1)\Theta_i - \Gamma - 1}{P(3\Gamma-1)\Theta_j - \Gamma - 1}, \tag{2}$$

for the vector and planar cases, respectively. These equations include $\Theta = \cos(\theta)^2$, where θ is x-ray incidence angle, with normal to the surface being 90°, $A = \cos(\alpha)^2$ or $\Gamma = \cos(\gamma)^2$, where α and γ are the angles between the vector or plane normal and the surface normal, and P is the degree of linear polarization. The $I_v(\Theta_i, A)$ and/or $I_p(\Theta_i, \Gamma)$ are intensities of

resonances acquired at various incident angles, Θ_i and Θ_j, and appear as a ratio in order to cancel both the intrinsic and experimental polarization-independent cross-section of the resonance. In practice, Eqs. (1) and (2) are linear functions of Θ_i, using any chosen and fixed Θ_j.

The StoBe DFT code[32] enables simulation of the x-ray absorption, the angular dependence of the intensities of NEXAFS resonances, as well as assignment of the unoccupied/final-state orbitals responsible for the NEXAFS resonances. In condensed films of PCs, inter-molecular forces consist primarily of weak van der Waals interactions; consequently, the ensemble is closely approximated by application of DFT to isolated PCs. To model the C and N K-edges, the standard StoBe approach is used to calculate the absorption from each respective atomic center by placing an extended and diffuse iii_iglo basis set on the atom of interest and pseudopotentials, approximating the two 1s core electrons, on all other atomic centers.[67] The computation of the x-ray spectrum at each atomic center required three steps: (1) relaxation of the molecular structure, and computation of the ground state; (2) calculation of the transition potential (TP), in which incorporation of a fractional (usually 1/2) electronic charge in the alpha spin state of the 1s core-electron was used to compute the profile of the x-ray absorption, statically approximating the dynamic initial and final state; and (3) recomputation of the energy levels with a core-hole in the alpha spin state of the 1s, and an electron in what was the LUMO of the ground state. Finally, the energy scale of the TP computed spectra was adjusted such that the energy of the first resonance matched the overall energy difference between the core-hole state and ground state.[67] No further adjustments were made to the energy scales.

Angular dependence of the intensities of NEXAFS resonances was simulated using the xrayspec utility included in the StoBe package along with an auxiliary, self-written code to compute electric field vectors for each angle of incidence and atomic center. Molecular three-fold azimuthal symmetry is sufficient to compute spectra with multiple azimuthal orientations and domain sizes much smaller than the experimental x-ray beam spot.[35] For a given polar molecular orientation and angle of x-ray incidence (with respect to the substrate surface), electric field vectors were calculated and fed into the xrayspec code. The results were summed over all C (or alternatively all N) centers to obtain the angular-dependent NEXAFS spectra. Modeling of the metal L-edges in Co-, Fe-, and Cu- PCs with StoBe proved to be more challenging than C and N K-edges. Other methods are often used to compute x-ray spectra from higher-Z atomic centers[68–71]; however, StoBe, which is a real-space, Gaussian-type-orbital code proved adequate to illuminate the nature of the unoccupied orbitals responsible for the most prominent experimentally observed resonances and the dependence of their intensities on the angle of incidence between the molecule and the x-ray beam. Simulations of NEXAFS by the StoBe code most often use a fractional charge of about 1/2 in the 1s core-level; to achieve approximately 1/2 of an electronic charge in the 2p core-level for the TP calculation, each of the three 2p alpha orbitals was assigned an occupation of 0.833.[72] The angular dependence and/or orbital overlap between the occupied and unoccupied states is expected to be different whether the initial state is an in-plane orbital (p_x or p_y) or an out-of-plane (p_z) orbital, and therefore, all three p-orbital orientations were explicitly included in the computed x-ray absorption. Further, the most likely oxidation state and electronic structure in square-planar Cu phthalocyanine is well established to be Cu^{2+} with a singly occupied $b_{1g}/d_{x^2-y^2}$ at the HOMO and LUMO.[73] As StoBe apparently uses alpha spin states for computation of x-ray absorption, we used two methods to ensure appropriate empty LUMO states in odd-electron (Cu and Co PC) systems: first, computation of cations with this single electron removed, and second, shown here, explicitly forcing the extra electron to be in a beta state. Both methods gave quantitatively similar results. Also, the resultant HOMO and LUMO states in the metal edges, as well as energetic ordering in, for example, N K-edges in Cu PC[52] were highly dependent on core-level fractional charge and proper SCF convergence was very sensitive to mixing, direct inversion of the iterative subspace parameters, and level shifting the unoccupied states.[32] The results of our approach, especially in the Cu-phthalocyanine L-edge, matched experimental spectra.

RESULTS

Figure 2 presents representative C K-edge NEXAFS spectra for Cu-phthalocyanine films deposited on sapphire as a function of the angle of x-ray incidence with respect to the sapphire surface. These spectra are representative of the other PCs measured during the course of this study. In this case, the intensities of the most prominent π^* resonances (labeled) are more intense at normal incidence than at grazing incidence. Analysis of these π^* resonance intensities yields transition dipole moments that exceed 70° with respect to the sapphire surface normal. As these π^* resonances have transition dipole moments that are perpendicular to the phthalocyanine plane, this analysis indicates an upright orientation that is, on average, within 20° of the surface normal for the Cu-phthalocyanine when deposited on sapphire.

Figure 3 presents representative C K-edge NEXAFS spectra for the four investigated phthalocyanines prepared on Au substrates. Each contains two prominent π^* resonances

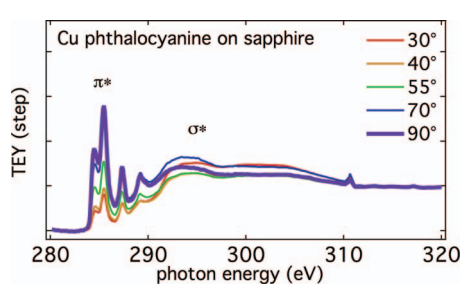

FIG. 2. Carbon NEXAFS from Cu phthalocyanine on sapphire. The two most prominent π^* resonances, about 284.5 and 285.5 eV are most intense at normal incidence, least at grazing, indicating an upright orientation of the phthalocyanines. The feature at about 310 eV is beamline artifact and/or contaminant.

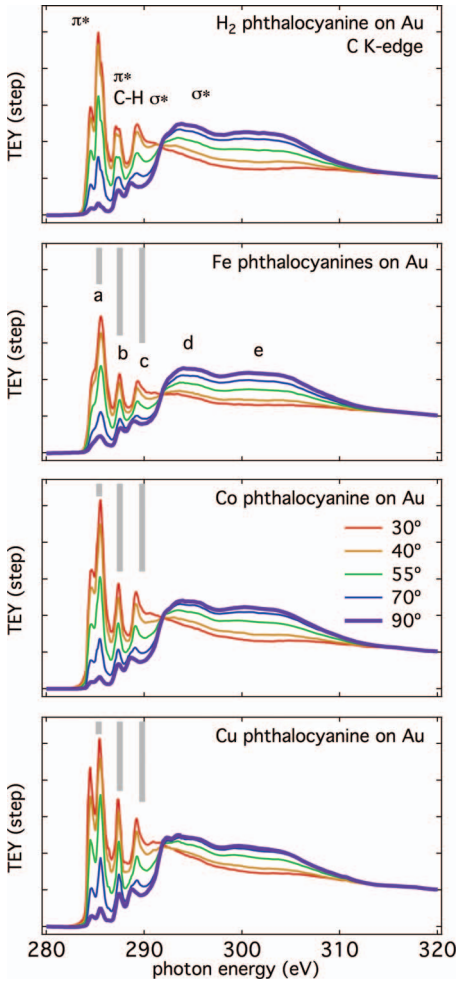

FIG. 3. Carbon K-edge NEXAFS from, top to bottom, H_2, Fe, Co, and Cu phthalocyanines on Au. All exhibit π^* and σ^* angular dependence that indicates, in these cases on Au, the planar molecules lie prostrate on the substrates. Features a-e are labeled in the Fe-PC pane; similar peaks are found in the other films with gray bars as a guide to the eye for the major manifolds of π^* common to all phthalocyanines.

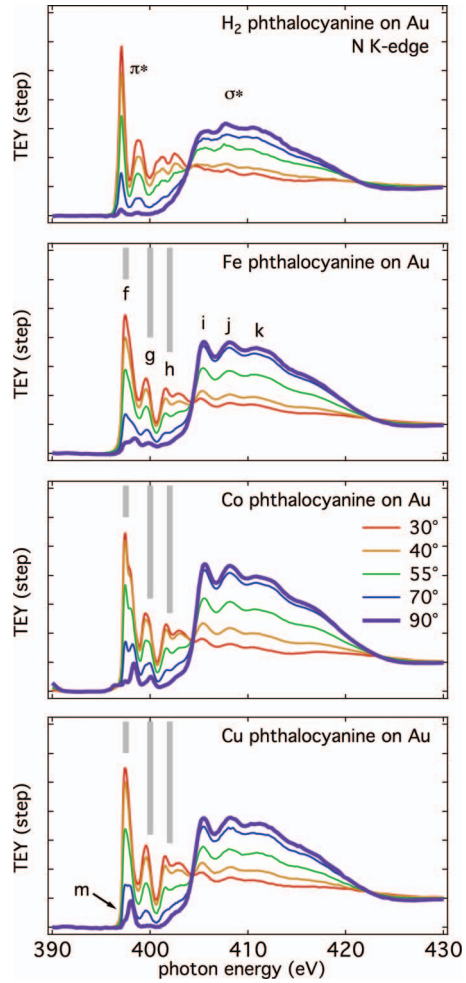

FIG. 4. Nitrogen K-edge NEXAFS spectra for each of the H_2, Fe, Co, and Cu phthalocyanine thin films on Au show π^* and σ^* angular dependence similar to the C K-edge spectra. Subtle differences between N and C K-edges are discussed in the text. Gray bars serve as a guide to the eye for π^* common to all spectra.

(a in Fig. 3) at about 284.5 and 285.5 eV. In contrast with Figure 2, these π^* resonances are most intense at grazing incidence, where the electric field of the incident radiation is near normal to the surface and PC thin film. Several additional features at energies just below the absorption edge (287–290 eV, labeled (b) and (c) in Fig. 3) have contributions from both π^* states and C−H bonding. Above the absorption edge (∼291.8 eV), the spectra from carbonaceous molecules are generally dominated by in-plane C−C and C−N σ^* features (d and e). The σ^* features in Figure 3 are generally most intense at normal incidence, and least prominent at grazing incidence. All resonances consistently increase monotonically (π^*) or decrease (σ^*) as the x-ray incidence angle is adjusted from normal to grazing, suggesting high fidelity in these measurements.

Figure 4 displays N K-edge NEXAFS spectra for thin films prepared from all four of the phthalocyanine complexes on Au; as expected, there are strong similarities in angular dependence between the N and C K-edge spectra. The π^* resonance manifolds (f, g, and h) are extremely intense at grazing incidence, while at normal incidence they are relatively weak. In the particular case of the H_2-phthalocyanine film, the π^* resonance (f) is nearly two orders of magnitude less intense at normal incidence (90°) than at grazing incidence (30°). The σ^* (i, j, and k) are most intense at normal incidence.

The NEXAFS spectra presented in Figures 3 and 4 indicate completely flat and prostrate orientations of all molecules are well within the error (one standard deviation) of the linear fit of Eq. (1) at the N K-edge π^*, with the exception of Fe-PC being within two standard deviations.[52] The deconvoluted σ^* (i, j, and k in Fig. 4) also return a highly prostrate orientation.[52] This is in direct contrast, and potentially an improvement over, previous studies where often a prostrate monolayer at the substrate interface is followed by upright phthalocyanines in thicker films.[16,22,23,29,38] With the deposition conditions used here, a homogeneously prostrate orientation is measured in phthalocyanine films on Au substrates as seen in the C and N K-edge data. Finally, the resonances above the absorption edge, namely i, j, and k, are more distinct in the metal PC films than with the H_2-PC films; thus, we infer that these resonances are influenced by N orbital overlap

with the metals. These quantitatively and uniformly flat orientations provide a platform to study angular-dependent resonances in organometallic phthalocyanine from films consisting of molecules with uniformly flat orientations.

Subtle differences exist between the N K-edge and C K-edge spectra. The manifold of resonances just below the absorption edge in the N K-edge data (h) are primarily π^* resonances. At most, only two of the eight N atoms, exclusively in the case of H_2-PC, are terminated with H. In contrast, the analogous region (c in Fig. 3) in the C K-edge has a convolution of both π^* and C−H σ^* resonances, resulting in some intensity in this region at normal x-ray incidence. This C−H σ^* intensity arises because 50% of the C atoms reside at the perimeter of the PC molecule and, consequently, are bonded to H (Fig. 1). All of the PCs contain a manifold of low energy resonances (f) that generally have angular dependence consistent with π^* resonances; however, specifically in the metal PCs, a relatively sharp resonance persists at normal incidence, for example (m) in CuPC, and exhibits the opposite angular dependence compared to the π^* resonances. This feature is evident in all metal PCs, particularly for Co- and Cu- PCs.

NEXAFS data recorded as a function of incidence angle at the metal spin-orbit split $L_{3,2}$-edges are presented in Figure 5. All display strong angular dependence, yet distinct features are apparent between the spectra for the three metal PC films. Both the lower-energy L_3 and higher-energy L_2 portions of the spectra from Fe- and Co- PC films exhibit angular dependence similar to the N and C K-edges: strong resonances at lower energies homologous with C/N π^* resonances (p in Fig. 5), and higher energy, broader resonances analogous to the C−C/N−C σ^* features (q) at both the L_3- and L_2- edges. The most pronounced difference between the Fe- and Co- PC NEXAFS spectra is the presence of a single, sharp resonance that appears at the onset of absorption only at the Fe-PC L_3-edge (n in Fig. 5), which has been attributed to a magnetic state.[4] In stark contrast with the Fe- and Co-PC data, the Cu-PC spectra show the first sharp resonance (r in Fig. 5) with the opposite angular dependence (strongest at normal incidence, weakest at grazing). About 3.4 eV above this intense resonance (s in Fig. 5) appears a barely perceptible peak with slight angular dependence consistent with an out-of-plane resonance. A broader, higher-energy resonance (t in Fig. 5), at about 8 eV above the intense peak, although relatively weakly, also runs counter to the angular dependence of the in-plane resonances of the Fe- and Co- PCs. Even though the Fe-, Co-, and Cu- centers all lie in the same phthalocyanine square-planar environment, the vastly different angular dependence of the NEXAFS clearly indicates different electronic structure and bonding for the Cu-PC with respect to the Fe- and Co- PC.

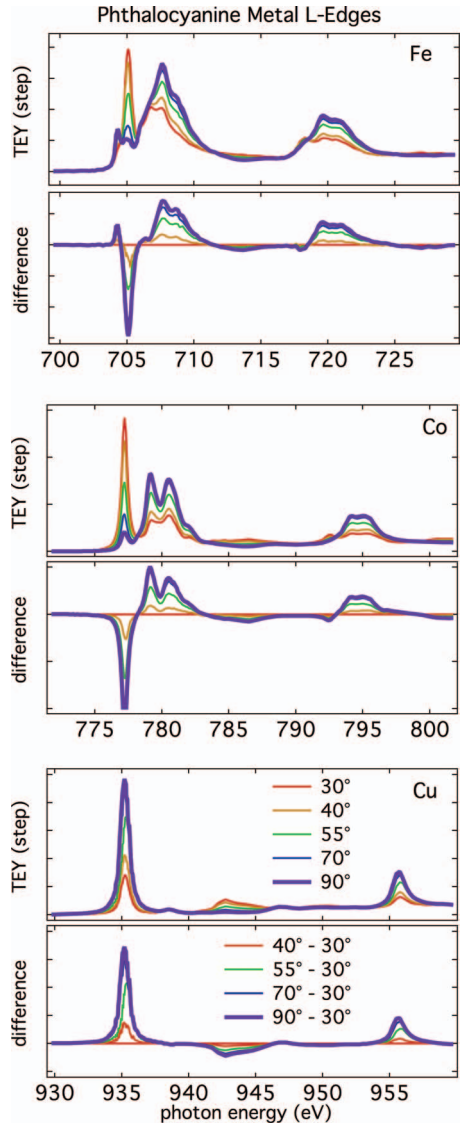

FIG. 5. NEXAFS spectra of metal $L_{2,3}$-edges from iron, cobalt, and copper phthalocyanines on Au. For each, both the total electron yield and difference are presented to emphasize the angular dependence of the resonances. Note distinctions between Fe, Co, and especially Cu spectra. Various features, labeled n-t, are described and interpreted in the text.

DISCUSSION

Angular dependent NEXAFS is an experimental measure of electronic structure; DFT calculations can help interpret and illuminate these data. The StoBe DFT code was used to this end, via simulation of the NEXAFS resonances and their observed angular dependence. Our assignments presented in the following paragraphs both confirm and contradict aspects of various assignments of features in the N and C K-edge made by previous observations and calculations.[26,36,39,51,62]

Generally, the most intense π^* resonances in the H_2-PC also appear in the metal PCs. In the N K-edge spectra of all four species, the lowest energy, most intense π^* resonance (f in Fig. 4) is composed of transitions from the 1s to LUMO e_g orbitals. These orbitals, some depicted in Fig. 6, are not simply localized at the pyrole rings[26]; but extend lengthwise across the two legs of the molecule. Each of these two orbitals involves all four of the peripheral N atoms,[36] but only two of the interior, pyrole N atoms. Thus, contributions to these resonances from peripheral N atoms are about twice as intense as from the interior nitrogens.[52] The next feature (g in Fig. 4) consists primarily of a convolution of a π^* state, which is delocalized over the entire molecule, and four π^* states at the benzene structures.[52]

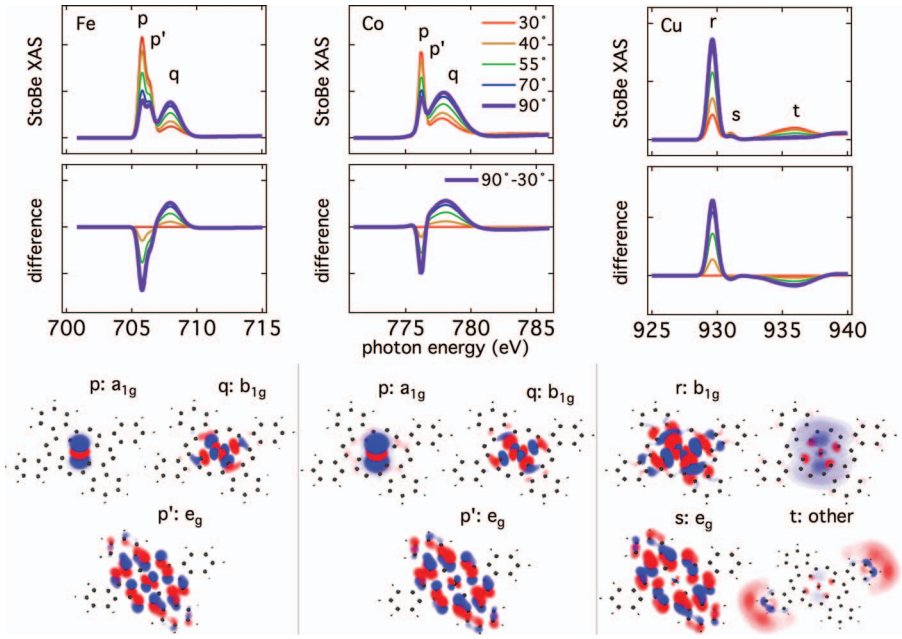

FIG. 6. StoBe computed L_3 edges for Fe, Co, and Cu phthalocyanines, as well as representative molecular orbitals responsible for the lowest-energy resonances.

Similar π^* resonances appear in the C K-edge spectra; however, the C features are a more complex convolution of transitions into unoccupied states shifted in energy by initial and final state differences than previously reported.[39] Phthalocyanine C atoms can be separated into two groups: pyrole C atoms within the 5 membered rings and bonded to two Ns, and benzene C atoms that are within the six-membered rings. The most intense C K-edge π^* resonance (a in Fig. 3) is a convolution of the LUMO e_g states excited from pyrole C, and the LUMO+1 states associated with benzene C structures, also excited from these same benzene C 1s levels. The shoulder/peak at about 1 eV lower energy (most distinct in Cu-PC, least distinct in Fe-PC) arises from transitions from benzene C into the LUMO e_g states. The next peak manifold (b in Fig. 3) is primarily an additional π^* state delocalized across much of the molecule. Further, additional states (manifold c in Fig. 3) are a mix of π^*, as well as σ^* character associated with C–H bonds.[52]

Figure 6 presents StoBe DFT computed NEXAFS spectra for the metal L_3-edges only, as well as diagrams of the molecular orbitals that correspond to the most prominent lowest-energy resonances. Although not all of the experimental features and precise energy positions are reproduced, the computed spectra, at least from the standpoint of angular dependence and relative energies, match trends in the experimental data. Generally, there are two manifolds of peaks, one a few eV higher than the first. The angular dependencies of the lowest energy features from the Fe- and Co- PC NEXAFS resonances are similar to experiment (p and q in Figs. 5 and 6), while the Cu-PC resonances, with opposite angular dependence, also resemble experiment (resonances r and t in Figs. 5 and 6).

The experimental NEXAFS for the Fe- and Co- PC films on Au possesses a strong, out-of-plane transition dipole moment (p in Fig. 5), resembling the π^* resonances observed at the C and N K-edges. The corresponding TP calculations confirm that the Fe-PC has a d_z^2 atomic-like/a_{1g} LUMO orbital[53] (p in Fig. 6) and then two e_g orbitals (with d_{xz} and d_{yz} character at the Fe central atom) in the LUMO+1 (p′ in Fig. 6); examples of these calculated orbitals are shown beneath the Fe computed spectrum.[52] All three orbitals, according to the calculation, contribute to the intensities of these lowest-energy resonances. The lowest-energy shoulder (n in Fig. 5) is not reproduced in our calculations, but we do note that the angular dependence is different whether the e_g resonance is excited from a $2p_x$ or $2p_y$ core-level compared to the $2p_z$, and this resonance has previously been attributed to an e_g state.[4] The Co-PC ground state exhibits a single unoccupied a_{1g} state[44]; in the StoBe TP calculation, both the a_{1g} and e_g resonances are responsible for its lowest-energy resonance, but the contribution from 2p into e_g states is relatively smaller than in Fe-PC. Both Fe- and Co- PCs thus have computed e_g orbitals that have d_{xz} and d_{yz} character near the metal center; these have been referred to as d-π because of the strong orbital overlap.[58] The next in-plane resonance for both Fe- and Co-PC (q) is due to an empty b_{1g} state. Although the transition dipole moments of L-edges are generally more complex than K-edges due to initial states with p-symmetry, experimentally, these particular 2p to $3d_z^2$, $3d_{xz}$, and $3d_{yz}$ resonances, probed with linearly polarized x-rays (Fig. 5), have angular dependence resembling the C and N 1s to molecular π^* states (Figs. 3 and 4). Conversely, the 2p to $3d_{x^2-y^2}$ resonance is in-plane and very analogous to σ^* resonances.

In stark contrast to the Fe- and Co- L-edges, the Cu-phthalocyanine lowest-energy peak is a strong in-plane resonance from the unoccupied b_{1g} orbital with $d_{x^2-y^2}$ character at the Cu atom; this orbital is also depicted below the computed spectra in Figure 6. The Cu 2p to $d_{x^2-y^2}$ assignment in phthalocyanines (and related molecules) is not without precedent; however, previous investigations neither distinguished

resonances into the same final state from the most intense C and/or N 1s to π^* transitions,[39,73,74] nor specifically looked experimentally for transitions to this final state in both N K-edges and Cu $L_{3,2}$ edges simultaneously.[49,62] Also, a relatively weak, but energetically sharp resonance in the N NEXAFS (m, Fig. 4) persists at normal incidence in the metal PCs. Deconvoluting this resonance from the spectra gives a precisely in-plane resonance for excitations from the N 1s into the $b_{1g}/d_{x^2-y^2}$ state[49,52] and also appears in the Fe- and Co-PCs (see Fig. 5). The energy position of this peak does not change as dramatically with metal atomic number in the experimental NEXAFS data compared to both our StoBe XAS simulations[52] and other ground-state calculations.[58]

The relative energy positions of the experimental resonances into e_g and b_{1g} orbitals are also highly dependent on the core-level used to probe these unoccupied states via x-ray absorption. As an example, in the Cu L_3 edge, the b_{1g} (r, Fig. 5) is about 3.2 eV *below* the e_g state (s, Fig. 5). In the Cu-PC N K-edge the positions are swapped: the b_{1g} (m in Fig. 4) lies 0.4 and 0.7 eV *above*, the two peaks fit to the lowest energy π^* manifold (f in Fig. 4).[52] This difference can only be due to the inherently dynamic nature of the x-ray absorption and differences in electron screening when the unoccupied state is probed from Cu 2p vs. N 1s core-electron.

Assignments can also be made to higher energy resonances in the Cu-PC. These computations support the assignment of feature s, 3.2 eV above the lowest-energy resonance, to the e_g orbitals[74] as depicted in Fig. 6, instead of into 4s states as tentatively stated previously.[73] The broader resonance, occurring 6.6–11.0 eV and labeled t, arises from several resonances with 4s and $4d_{z^2}$ character; two of the more prominent computed orbitals are depicted in Fig. 6.

CONCLUSIONS

Experimental and theoretical analysis of x-ray absorption in ordered thin films of H_2-, Fe-, Co-, and Cu- phthalocyanines at the C and N K-edges, and the respective metal L-edges has provided both the preferred molecular orientation within these condensed films and a detailed description of the associated electronic structure. Phthalocyanines deposited on sapphire studied in this work assume upright orientations through analysis of the angular dependence of resonances in the C and N K-edge NEXAFS. Conversely, on substrates consisting of 30 nm Au deposited on sapphire and annealed at 300 °C, these PCs lay prostrate on the surface. The Fe, Co, and Cu L-edge NEXAFS also show strong angular dependence, but vary significantly between the three species. Iron and cobalt PCs have angular dependence that resembles the C and N K-edges, with out-of-plane a_{1g} ($3d_{z^2}$) and e_g (d_{xy} d_{xz} or d-π^*) states dominating the lowest unoccupied orbitals, and at higher energy, transitions into the in-plane b_{1g} orbital which has $d_{x^2-y^2}$ character at the metal center. Conversely, the Cu L-edge exhibits a strong in-plane b_{1g} resonance. Weaker features at 3.2 eV and 6.6-10.0 eV higher energy, with out-of-plane angular dependence, are attributed to the e_g states, and various transitions into states with 4s and $4d_{z^2}$ character at the metal centers.

ACKNOWLEDGMENTS

Portions of this work performed under the auspices of the U.S. Department of Energy by Lawrence Livermore National Laboratory under Contract No. DE-AC52-07NA27344. The Advanced Light Source is supported by the Director, Office of Science, Office of Basic Energy Sciences, of the U.S. Department of Energy under Contract No. DE-AC02-05CH11231. Portions of this research were carried out at the Stanford Synchrotron Radiation Lightsource, a Directorate of SLAC National Accelerator Laboratory and an Office of Science User Facility operated for the U.S. Department of Energy Office of Science by Stanford University. This work was supported by a University of California Office of the President (UCOP) Management Fee Grant, "Carbon Nanostructures." The authors acknowledge Juan Bartolome, Franz Himpsel, Xiaosong Liu, and Ioannis Zegkinoglou for useful discussions. C.M. and I.V. acknowledge AFOSR FA 9550-10-1-0409.

[1] R. D. Gould, Coord. Chem. Rev. **156**, 237–274 (1996).
[2] C. N. Colesniuc, R. R. Biswas, S. A. Hevia, A. V. Balatsky, and I. K. Schuller, Phys. Rev. B **83**(8), 085414 (2011).
[3] M. Evangelisti, J. Bartolome, L. J. de Jongh, and G. Filoti, Phys. Rev. B **66**(14), 144410 (2002).
[4] J. Bartolome, F. Bartolome, L. M. Garcia, G. Filoti, T. Gredig, C. N. Colesniuc, I. K. Schuller, and J. C. Cezar, Phys. Rev. B **81**(19), 195405 (2010).
[5] C. W. Miller, A. Sharoni, G. Liu, C. N. Colesniuc, B. Fruhberger, and I. K. Schuller, Phys. Rev. B **72**(10), 104113 (2005).
[6] K. P. Gentry, T. Gredig, and I. K. Schuller, Phys. Rev. B **80**(17), 174118 (2009).
[7] J. B. MacNaughton, A. Moewes, J. S. Lee, S. D. Wettig, H. B. Kraatz, L. Z. Ouyang, W. Y. Ching, and E. Z. Kurmaev, J. Phys. Chem. B **110**(32), 15742–15748 (2006).
[8] A. W. Hains, Z. Q. Liang, M. A. Woodhouse, and B. A. Gregg, Chem. Rev. **110**(11), 6689–6735 (2010).
[9] R. D. Yang, T. Gredig, C. N. Colesniuc, J. Park, I. K. Schuller, W. C. Trogler, and A. C. Kummel, Appl. Phys. Lett. **90**(26), 263506 (2007).
[10] R. D. Yang, J. Park, C. N. Colesniuc, I. K. Schuller, W. C. Trogler, and A. C. Kummel, J. Appl. Phys. **102**(3), 034515 (2007).
[11] V. Y. Aristov, O. V. Molodtsova, Y. A. Ossipyan, B. P. Doyle, S. Nannarone, and M. Knupfer, Org. Electron. **10**(1), 8–11 (2009).
[12] J. Park, J. E. Royer, C. N. Colesniuc, F. I. Bohrer, A. Sharoni, S. H. Jin, I. K. Schuller, W. C. Trogler, and A. C. Kummel, J. Appl. Phys. **106**(3), 034505 (2009).
[13] R. D. Yang, J. Park, C. N. Colesniuc, I. K. Schuller, J. E. Royer, W. C. Trogler, and A. C. Kummel, J. Chem. Phys. **130**(16), 164703 (2009).
[14] K. A. Miller, R. D. Yang, M. J. Hale, J. Park, B. Fruhberger, C. N. Colesniuc, I. K. Schuller, A. C. Kummel, and W. C. Trogler, J. Phys. Chem. B **110**(1), 361–366 (2006).
[15] F. I. Bohrer, A. Sharoni, C. Colesniuc, J. Park, I. K. Schuller, A. C. Kummel, and W. C. Trogler, J. Am. Chem. Soc. **129**(17), 5640–5646 (2007).
[16] F. I. Bohrer, C. N. Colesniuc, J. Park, I. K. Schuller, A. C. Kummel, and W. C. Trogler, J. Am. Chem. Soc. **130**(12), 3712–3713 (2008).
[17] F. I. Bohrer, C. N. Colesniuc, J. Park, M. E. Ruidiaz, I. K. Schuller, A. C. Kummel, and W. C. Trogler, J. Am. Chem. Soc. **131**(2), 478–485 (2009).
[18] J. B. MacNaughton, M. V. Yablonskikh, A. H. Hunt, E. Z. Kurmaev, J. S. Lee, S. D. Wettig, and A. Moewes, Phys. Rev. B **74**(12), 125101 (2006).
[19] C. Monton, I. Valmianski, and I. K. Schuller, Appl. Phys. Lett. **101**(13), 133304 (2012).
[20] I. Biswas, H. Peisert, T. Schwieger, D. Dini, M. Hanack, M. Knupfer, T. Schmidt, and T. Chasse, J. Chem. Phys. **122**(6), 064710 (2005).
[21] I. Biswas, H. Peisert, L. Zhang, T. Chasse, M. Knupfer, M. Hanack, D. Dini, T. Schmidt, and D. Batchelor, Mol. Cryst. Liq. Cryst. **455**, 241–249 (2006).
[22] H. Peisert, I. Biswas, L. Zhang, M. Knupfer, M. Hanack, D. Dini, D. Batchelor, and T. Chasse, Surf. Sci. **600**(18), 4024–4029 (2006).
[23] I. Biswas, H. Peisert, M. Nagel, M. B. Casu, S. Schuppler, P. Nagel, E. Pellegrin, and T. Chasse, J. Chem. Phys. **126**(17), 174704 (2007).

[24]O. V. Molodtsova, V. Y. Aristov, V. M. Zhilin, Y. A. Ossipyan, D. V. Vyalikh, B. P. Doyle, S. Nannarone, and M. Knupfer, Appl. Surf. Sci. **254**(1), 99–102 (2007).
[25]O. V. Molodtsova, M. Knupfer, Y. A. Ossipyan, and V. Y. Aristov, J. Appl. Phys. **104**(8), 083704 (2008).
[26]A. Calabrese, L. Floreano, A. Verdini, C. Mariani, and M. G. Betti, Phys. Rev. B **79**(11), 115446 (2009).
[27]M. Grobosch, V. Y. Aristov, O. V. Molodtsova, C. Schmidt, B. P. Doyle, S. Nannarone, and M. Knupfer, J. Phys. Chem. C **113**(30), 13219–13222 (2009).
[28]J. Xiao and P. A. Dowben, J. Phys.: Condens. Matter **21**(5), 052001 (2009).
[29]H. Peisert, I. Biswas, M. Knupfer, and T. Chasse, Phys. Status Solidi B **246**(7), 1529–1545 (2009).
[30]G. Liu, T. Gredig, and I. K. Schuller, Europhys. Lett. **83**(5), 56001 (2008).
[31]R. G. Wilks, E. Z. Kurmaev, L. M. Sandratskii, A. V. Postnikov, L. D. Finkelstein, T. P. Surkova, S. A. Lopez-Rivera, and A. Moewes, J. Phys.: Condens. Matter **18**(46), 10405–10412 (2006).
[32]K. Hermann, L. G. M. Pettersson, M. E. Casida, C. Daul, A. Goursot, A. Koester, E. Proynov, A. St.-Amant, and D. R. Salahub, StoBe-deMon version 3.1 (2011).
[33]Z. H. Cheng, S. X. Du, W. Guo, L. Gao, Z. T. Deng, N. Jiang, H. M. Guo, H. Tang, and H. Gao, Nano Res. **4**(6), 523–530 (2011).
[34]M. V. Yablonskikh, J. Braun, M. T. Kuchel, A. V. Postnikov, J. D. Denlinger, E. I. Shreder, Y. M. Yarmoshenko, M. Neumann, and A. Moewes, Phys. Rev. B **74**(8), 085103 (2006).
[35]J. Stöhr, *NEXAFS Spectroscopy* (Springer-Verlag, Berlin-Heidelberg-New York, 1992).
[36]F. Evangelista, V. Carravetta, G. Stefani, B. Jansik, M. Alagia, S. Stranges, and A. Ruocco, J. Chem. Phys. **126**(12), 124709 (2007).
[37]T. M. Willey, A. L. Vance, T. van Buuren, C. Bostedt, A. J. Nelson, L. J. Terminello, and C. S. Fadley, Langmuir **20**(7), 2746–2752 (2004).
[38]H. Peisert, I. Biswas, L. Zhang, M. Knupfer, M. Hanack, D. Dini, M. J. Cook, I. Chambrier, T. Schmidt, D. Batchelor, and T. Chasse, Chem. Phys. Lett. **403**(1–3), 1–6 (2005).
[39]V. Y. Aristov, O. V. Molodtsova, V. Maslyuk, D. V. Vyalikh, V. M. Zhilin, Y. A. Ossipyan, T. Bredow, I. Mertig, and M. Knupfer, Appl. Surf. Sci. **254**(1), 20–25 (2007).
[40]V. Y. Aristov, O. V. Molodtsova, V. V. Maslyuk, D. V. Vyalikh, V. M. Zhilin, Y. A. Ossipyan, T. Bredow, I. Mertig, and M. Knupfer, J. Chem. Phys. **128**(3), 034703 (2008).
[41]P. L. Cook, W. L. Yang, X. S. Liu, J. M. Garcia-Lastra, A. Rubio, and F. J. Himpsel, J. Chem. Phys. **134**(20), 204707 (2011).
[42]M. L. M. Rocco, K. H. Frank, P. Yannoulis, and E. E. Koch, J. Chem. Phys. **93**(9), 6859–6864 (1990).
[43]E. E. Koch, Y. Jugnet, and F. J. Himpsel, Chem. Phys. Lett. **116**(1), 7–11 (1985).
[44]T. Kroll, V. Y. Aristov, O. V. Molodtsova, Y. A. Ossipyan, D. V. Vyalikh, B. Buchner, and M. Knupfer, J. Phys. Chem. A **113**(31), 8917–8922 (2009).
[45]L. Zhang, H. Peisert, I. Biswas, M. Knupfer, D. Batchelor, and T. Chasse, Surf. Sci. **596**(1–3), 98–107 (2005).
[46]A. Rosa and E. J. Baerends, Inorg. Chem. **33**, 584–595 (1994).
[47]B. N. Holland, G. Cabailh, N. Peltekis, C. McGuinness, A. A. Cafolla, and I. T. McGovern, Appl. Surf. Sci. **255**(3), 775–777 (2008).
[48]O. V. Molodtsova, M. Knupfer, V. Y. Aristov, D. V. Vyalikh, V. M. Zhilin, and Y. A. Ossipyan, J. Appl. Phys. **103**(5), 053711 (2008).
[49]B. N. Holland, N. Peltekis, T. Farrelly, R. G. Wilks, G. Gavrila, D. R. T. Zahn, C. McGuinness, and I. T. McGovern, Phys. Status Solidi B **246**(7), 1546–1551 (2009).
[50]J. M. Garcia-Lastra, P. L. Cook, F. J. Himpsel, and A. Rubio, J. Chem. Phys. **133**(15), 151103 (2010).
[51]M. Linares, S. Stafstrom, Z. Rinkevicius, H. Agren, and P. Norman, J. Phys. Chem. B **115**(18), 5096–5102 (2011).
[52]See supplementary material at http://dx.doi.org/10.1063/1.4811487 which contains computational method templates, computed spectra and associated orbitals, peakfitting, and angular dependence of various deconvoluted resonances.
[53]T. Kroll, R. Kraus, R. Schonfelder, V. Y. Aristov, O. V. Molodtsova, P. Hoffmann, and M. Knupfer, J. Chem. Phys. **137**(5), 054306 (2012).
[54]S. Stepanow, P. S. Miedema, A. Mugarza, G. Ceballos, P. Moras, J. C. Cezar, C. Carbone, F. M. F. de Groot, and P. Gambardella, Phys. Rev. B **83**(22), 220401 (2011).
[55]G. Dufour, C. Poncey, F. Rochet, H. Roulet, M. Sacchi, M. Desantis, and M. Decrescenzi, Surf. Sci. **319**(3), 251–266 (1994).
[56]M. G. Betti, P. Gargiani, R. Frisenda, R. Biagi, A. Cossaro, A. Verdini, L. Floreano, and C. Mariani, J. Phys. Chem. C **114**(49), 21638–21644 (2010).
[57]T. Hamilton, M. Foursa, A. Hirose, and A. Moewes, Radiat. Phys. Chem. **75**(11), 1613–1616 (2006).
[58]M. S. Liao and S. Scheiner, J. Chem. Phys. **117**(1), 205–219 (2002).
[59]L. Lozzi, S. Santucci, S. La Rosa, B. Delley, and S. Picozzi, J. Chem. Phys. **121**(4), 1883–1889 (2004).
[60]J. B. MacNaughton, R. G. Wilks, J. S. Lee, and A. Moewes, J. Phys. Chem. B **110**(37), 18180–18190 (2006).
[61]J. H. Seo, D. S. Park, S. W. Cho, C. Y. Kim, W. C. Jang, C. N. Whang, K. H. Yoo, G. S. Chang, T. Pedersen, A. Moewes, K. H. Chae, and S. J. Cho, Appl. Phys. Lett. **89**(16), 163505 (2006).
[62]O. V. Molodtsova, M. Knupfer, V. V. Maslyuk, D. V. Vyalikh, V. M. Zhilin, Y. A. Ossipyan, T. Bredow, I. Mertig, and V. Y. Aristov, J. Chem. Phys. **129**(15), 154705 (2008).
[63]V. V. Maslyuk, V. Y. Aristov, O. V. Molodtsova, D. V. Vyalikh, V. M. Zhilin, Y. A. Ossipyan, T. Bredow, I. Mertig, and M. Knupfer, Appl. Phys. A **94**(3), 485–489 (2009).
[64]G. S. Chang, E. Z. Kurmaev, L. D. Finkelstein, N. A. Babushkina, A. Moewes, and T. A. Callcott, Phys. Rev. B **74**(12), 125105 (2006).
[65]P. S. Miedema, S. Stepanow, P. Gambardella, and F. M. F. de Groot, J. Phys. Conf. Ser. **190**, 012143 (2009).
[66]C. N. Colesniuc, PhD dissertation (University of California, San Diego, 2011).
[67]M. Leetmaa, M. Ljungberg, H. Ogasawara, M. Odelius, L. A. Naslund, A. Nilsson, and L. G. M. Pettersson, J. Chem. Phys. **125**(24), 244510 (2006).
[68]J. J. Rehr and R. C. Albers, Rev. Mod. Phys. **72**(3), 621–654 (2000).
[69]J. J. Rehr, J. J. Kas, F. D. Vila, M. P. Prange, and K. Jorissen, Phys. Chem. Chem. Phys. **12**(21), 5503–5513 (2010).
[70]T. Anniyev, H. Ogasawara, M. P. Ljungberg, K. T. Wikfeldt, J. B. MacNaughton, L. A. Naslund, U. Bergmann, S. Koh, P. Strasser, L. G. M. Pettersson, and A. Nilsson, Phys. Chem. Chem. Phys. **12**(21), 5694–5700 (2010).
[71]F. de Groot, Coord. Chem. Rev. **249**(1–2), 31–63 (2005).
[72]R. G. Wilks, J. B. MacNaughton, H. B. Kraatz, T. Regier, and A. Moewes, J. Phys. Chem. B **110**(12), 5955–5965 (2006).
[73]G. Dufour, C. Poncey, F. Rochet, H. Roulet, S. Iacobucci, M. Sacchi, F. Yubero, N. Motta, M. N. Piancastelli, A. Sgarlata, and M. DeCrescenzi, J. Electron Spectrosc. Relat. Phenom. **76**, 219–224 (1995).
[74]S. Carniato, Y. Luo, and H. Agren, Phys. Rev. B **63**(8), 085105 (2001).